Quantification of the Microstructures of Hypoeutectic White Cast Iron using Mathematical Morphology and an Artificial Neuronal Network

Victor Albuquerque, João Manuel R. S. Tavares, Paulo Cortez

Abstract

This paper describes an automatic system for segmentation and quantification of the microstructures of white cast iron. Mathematical morphology algorithms are used to segment the microstructures in the input images, which are later identified and quantified by an artificial neuronal network. A new computational system was developed because ordinary software could not segment the microstructures of this cast iron correctly, which is composed of cementite, pearlite and ledeburite. For validation purpose, 30 samples were analyzed. The microstructures of the material in analysis were adequately segmented and quantified, which did not happen when we used ordinary commercial software. Therefore, the proposed system offers researchers, engineers, specialists and others, a valuable and competent tool for automatic and efficient microstructural analysis from images.

Keywords: hypoeutectic white cast iron, image processing and analysis, mathematical morphology, artificial neuronal network, image quantification.

1. Introduction

Cast iron is an iron-carbon-silicon alloy used in numerous industrial applications, such as the base structures of manufacturing machines, rollers, valves, pump bodies and mechanical gears, among others. The main families of cast irons are: nodular cast iron, malleable cast iron, grey cast iron and white cast iron (Callister, 2006). Their properties, as of all materials, are influenced by their microstructures and therefore, the correct characterization of their microstructures is highly important. Thus, quantitative metallography is commonly used to determine the quantity, appearance, size and distribution of the phases and constituents of the white cast iron microstructures. To carry this out, segmentation and quantification of the microstructures from metallographic images is usually done.

The main objective of the image segmentation process is to subdivide an original image into its component parts or objects. This is one of the earliest tasks of many computational systems used for image analysis. The level to which this subdivision must be carried out depends on the final objective to be reached from the original images. The segmentation process is finished when the objects of interest are correctly identified (Gonzalez and Woods, 2008).

Manual quantitative metallography, based on human visual inspection, is very tiring due to long periods that a specialist is exposed to high-luminosity in the microscope, which can cause fatigue and, consequently, increase the probability of measurement errors. To automate this archaic but still very common task, Computational Vision systems are being developed in order to optimize the quantification process, generating more precise results in a shorter time (Albuquerque et al., 2008; Albuquerque et al., 2009). However, using the more ordinary systems currently available, the quantification of some elements of the microstructures is frequently done incorrectly. For example, the constituents of ledeburite, which are austenite and cementite for the ledebutite I or pearlite and cementite for the ledebutite II, are segmented and quantified independently. Additionally, these systems usually set the threshold value to be

used in the segmentation of the microstructures manually, which can be very difficult to define in many cases, in particular by less experienced users.

This paper presents an innovative computational system for the analysis of images of ferrous alloys, which optimizes the process of segmentation and quantification of microstructures by using mathematical morphology and an artificial neural network. These are powerful techniques of digital image processing and artificial intelligence.

The next section presents the morphological operators considered: erosion, dilation, closing and opening. Following, the Artificial Neuronal Network (ANN) used is introduced. Subsequently, the system architecture is presented. Afterward, in section 5, some experimental results are shown and discussed. Finally, in the last section, the main conclusions are addressed.

2. Morphological operators

Morphological operators are very important tools in image processing. Erosion, dilation, opening and closing are the most commonly used operators.

2.1. Erosion and dilation

Consider that A and B are two non-empty sets where A represents the image in analysis and B the structure element to be used. Mathematically, the binary erosion for the A and B sets in Z^2 is defined by $A\theta B = \{Z|(B)z \subseteq A\}$. This operation is characterized by the reduction of the white pixels present in the input image (Gonzalez and Woods, 2008).

The binary dilation for the A and B sets in Z^2 is defined by $A \oplus B = \{Z|[(\hat{B})z \cap A] \subseteq A\}$, which results in the expansion of the white pixels present in the input image (Gonzalez and Woods, 2008).

As an illustrative example, Figure 1 shows the original image of a cast iron nodular, the correspondent binarized image and the resultant images of the erosion and dilation operators on the binarized image.

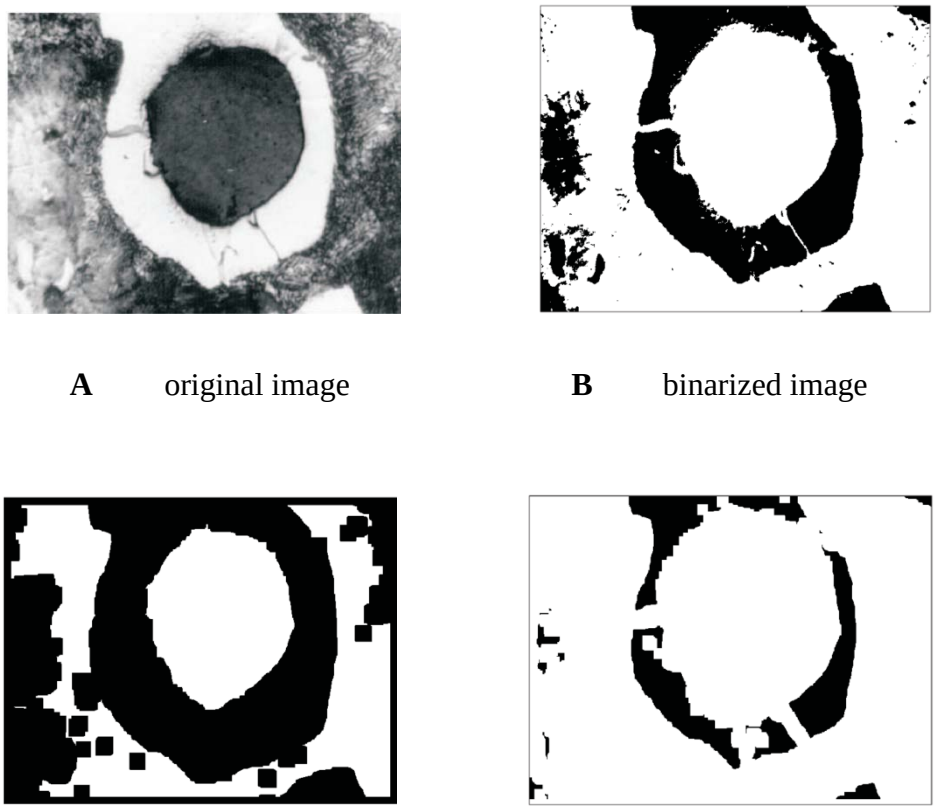

A original image **B** binarized image

C eroded image **D** dilated image

Fig. 1 Use of erosion and dilation operators on a binary image.

A original image

B binarized image

C eroded image

D dilated image

When the morphological dilation and erosion operators are applied one after the other to an input image, some of its main characteristics are enhanced. These then allow the construction of more important operators such as the morphological opening and closing operators, among others.

2.2. Opening and closing

The binary opening of a set A by B is defined as the erosion of A by B followed by the dilation of the result by B, and it is expressed as $A \circ B = (A \theta B) \oplus B$. It causes the smoothing of the shapes represented in the input images, eliminating small protuberances (Gonzalez and Woods, 2008).

Inverting the order of the operations that define the opening or, in other words, making the dilation of A by B, followed by the erosion of the result by B, produces the operation of closing, which can be expressed as $A \bullet B = (A \oplus B) \theta B$. It results in the filling of small holes and/or gaps in the shapes present in the input images (Gonzalez and Woods, 2008).

For a better understanding of the use of these operations, Figure 2 presents the results obtained by the closing and opening operations on the image of Figure 1b.

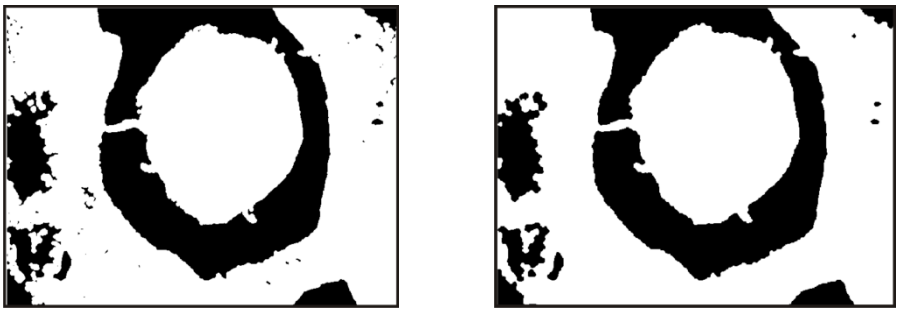

A closed image **B** opened image

Fig. 2 Use of closing and opening operators on a binary image (Figure 1b).

A closed image

B opened image

3. Artificial Neuronal Network

Artificial neuronal networks can be applied to problems of function approximation and classification, among others, as well as in cases with nonlinear interactions between the dependent variables and the independent ones. Nowadays, ANN are already being used in the

field of material science for welding control (Bhadeshia, 1999), to obtain the relations between process parameters and correlations in Charpy impact tests (Bhadeshia, 1994), to get the composition of models for ceramic matrices (Bhadeshia, 1999), in the modeling of alloy elements (Miaoquan et al., 2002; Miaoquan et al., 2003), in the prediction of welding parameters in pipeline welding (Kim et al., 2003), to model the microstructures and mechanical properties of steel (Kusiak and Kuziak, 2003), to model the deformation mechanism of titanium alloy in hot forming (Li and Miaoquan, 2005), for the prediction of properties of austempered ductile iron (Biernacki et al., 2006), to predict the carbon contents and the grain size of carbon steels (Abdelhay, 2005), to build models for predicting the flow stress and microstructural evolution of a hydrogenized titanium alloy (Wang et al., 2007), among other possible applications.

The fundamental paradigm of the ANN is to construct a composed model using a considerable number of units, which are called neurons and constitute a very simple processing unit, with a great number of connections between them. The information among the neurons employed in the network is transmitted through the synaptic weights.

The flexibility of the ANN, their capacity to learn from examples and to generalize the information learned are very attractive and important aspects that justify the choice of these tools for modeling many complex problems. In fact, the capacity of generalization and learning from a set of examples representative of the problem to be modeled, associated with the ability of supplying correct adjustments to input data that was not presented in the training phase, provides evidence of the capacity of the ANN to go further than the obvious relations between inputs and outputs. Given these abilities, the neural networks were capable of extracting information not presented in explicit forms in the training examples considered (Samarasinghe, 2006).

Several different topologies and algorithms of ANN can be found in the literature. In the proposed system, a back-propagation neural network of the feed-forward type (Haykin, 1994) is employed. This multilayer neural network is composed of several layers typically lined up with neurons. The input data is fed into the first layer, which distributes it through the internal hidden or intermediate layers. The last layer is an output layer, from which the solution of the problem is obtained. In most applications, just one hidden layer is considered.

Figure 3 presents the topology of the artificial neuronal network used: it has one input layer with three neurons, one hidden layer with two neurons and one output layer with three neurons.

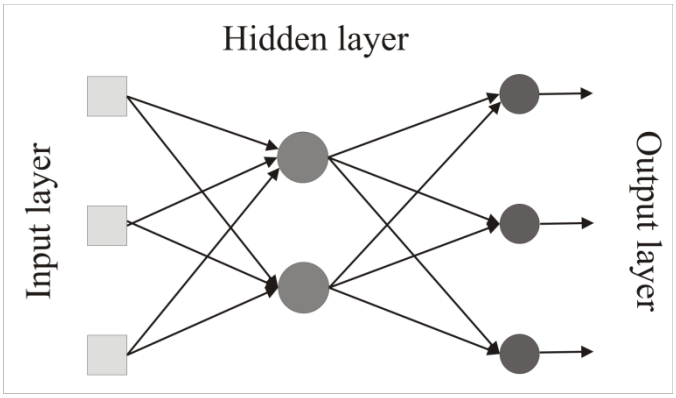

Fig. 3 Topology of the Artificial Neuronal Network used.

4. System developed

The process of segmenting and quantifying the microstructural elements from images integrated in the computational system developed can be described as follows:

The histogram of the image to be analyzed is obtained in order to automatically define the most adequate threshold level to be used in its binarization. Then, the input image is binarized and the morphological operators of closing and opening, using a structural element of the point type, are applied to the binarized image.

Afterwards, the morphological erosion operation is done three times to eliminate the pearlite globules and then the dilation morphological operation is applied, also three times, in order to segment the pearlite. This number of applications of the morphological operators gave the best results during our experimental tests and is a function of the size of the pearlite globules. Then, in order to get the cementite, the resultant image is inverted.

Finally, to segment the ledeburite, a subtraction of the image dilated from the binarized image is performed. As the ledeburite is presented in the form of small globules, there is the necessity of alternately applying the morphological operations of dilation, erosion, opening and closing, until a satisfactory segmentation is accomplished. The sequence of operators and the number that each operator is applied are again a function of the material under analysis.

After the segmentation of the microstructural elements of the white cast iron from the input image using mathematical morphology, their identification and quantification are made using the ANN.

Figure 4 shows the sequence of tasks to accomplish the quantification of the microstructures of a cast iron using the system developed in C/C++. The time needed to perform microstructures quantification from a metallographic image using our system is around 3 minutes considering only one sample, including the image acquisition step and using a PC with a Intel Core 2 Duo at 2.1 GHz, 2048 MB of RAM and running Microsoft Windows XP, while the same manual analysis needs around 2.5 to 3 hours depending on the operator’s experience.

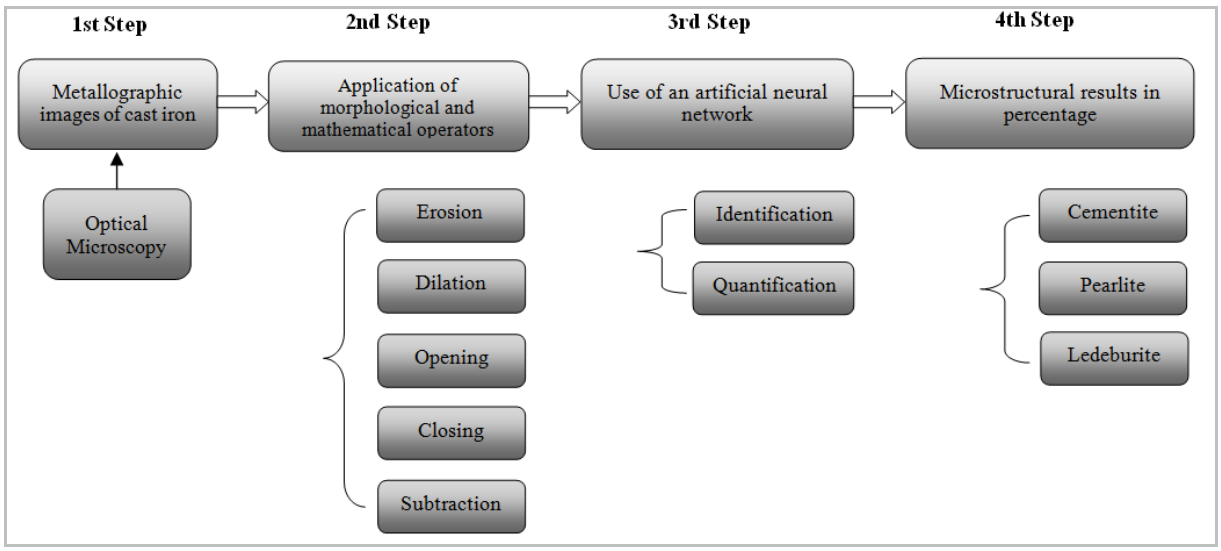

Fig. 4 Sequence of tasks to accomplish the quantification of the microstructures of a cast iron using the proposed system.

5. Experimental results

As previously mentioned, the microstructural elements of the white cast iron are not always segmented correctly by ordinary software. In fact, the ledeburite, composed of pearlite globules and cementite, Figure 5a, has been quantified incorrectly as the pearlite globules and the cementite (with blue color) have been segmented as independent elements, Figure 5b.

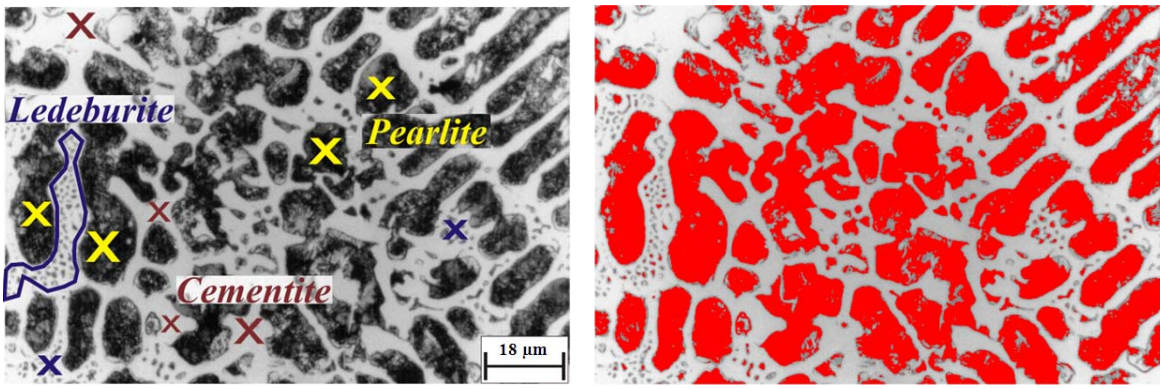

A original image **B** segmentation using ordinary software

Fig. 5 An original image of a white cast iron and the segmentation using ordinary software.

A original image

B segmentation using ordinary software

Our experimental tests were carried out using 30 samples of a white cast iron. From these 30 samples, one was used in this paper to illustrate the application of the proposed system for the segmentation and quantification of the microstructural elements from images, but all the results obtained were similar.

Figure 6 shows the histogram of the sample image, which is used to obtain the best threshold level to be applied in the binarization step. In the histogram, there is a valley, a characteristic of white cast irons, located to the left of the peak. The lower value in this valley corresponds to the best threshold level that should be used in the binarization of the associated image. The location of such a valley in the histogram is automatically determined by the system and the lowest value is detected and used as the threshold level for binarization. In the present case, the threshold level determined was 153.

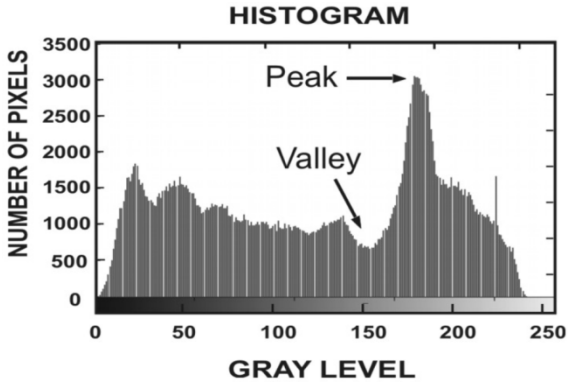

Fig. 6 Histogram of the Figure 5a image.

The pixels of the input image whose grey value is between zero and the threshold value found (in the present example, 153) represent the cementite microstructure, while the pixels above the threshold value are considered as being part of the pearlite microstructure.

Figure 7 presents the result accomplished by the binarization of the Figure 5a image of using the threshold value automatically obtained.

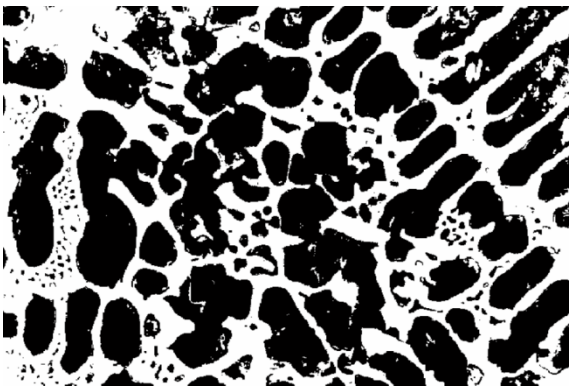

Fig. 7 Resultant image of the binarization process of the Figure 5a image.

Figure 8a presents the result of the application of the morphological closing operation. It is possible to see the dilation of the internal region of the pearlite and the maintenance of the size of the pearlite globules. Furthermore, Figure 8b presents the result of the application of

the opening operation. In this image, one can see a small erosion of the pearlite and a great reduction of pearlite globules and consequently a decrease of ledeburite.

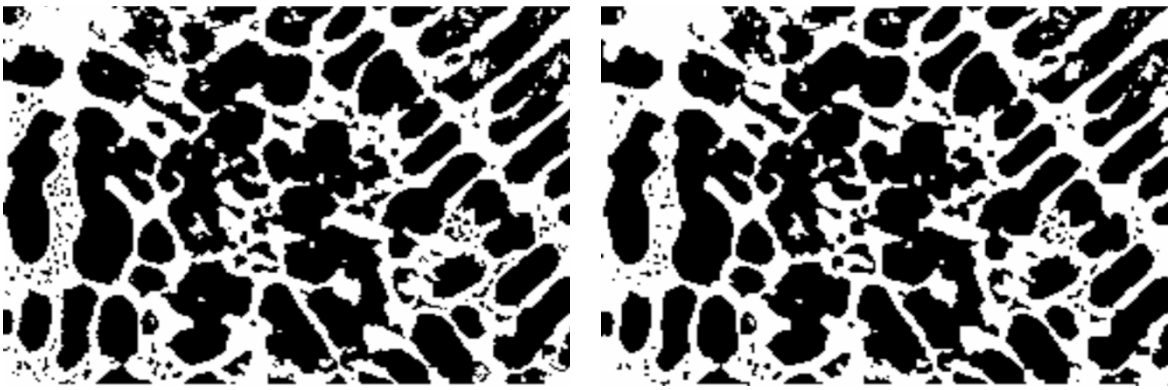

A result of closing **B** result of opening

Fig. 8 Results of closing and opening operators on the Figure 7 image.

A result of closing

B result of opening

Figures 9a and 9b present the results of erosion and dilation operations, respectively, applied on the resultant image of the opening operation, as seen in Figure 8b. In the eroded image a reduction of the pearlite and the elimination of pearlite globules can be seen. The reduction effect is then eliminated through a dilation operation using the same structure element that was previously used in the erosion. Therefore, this procedure recovers the reduced region of pearlite, keeping the elimination of pearlite globules and consequently, it is possible to obtain an adequate segmentation of pearlite and cementite, represented in black and white, respectively, as can be seen in Figure 9.

A result of erosion **B** result of dilation

Fig. 9 Results of erosion morphological operator on the Figure 8b image and dilation morphological operator on the Figure 9a image to segment the pearlite and cementite.

A result of erosion

B result of dilation

Figure 10a presents the result of the subtraction of the dilated image (Figure 9b) from the binarized image (Figure 6), with the pearlite globules easily visible (represented by black pixels). Figure 10b shows the result of the ledeburite segmentation (represented in black) through the applications of the morphological operations of opening (applied once), closing (applied twice), erosion (applied twice) and dilation (applied five times).

A result of subtraction **B** result of dilation

Fig. 10 Results of the subtraction and dilation operations in order to segment the ledeburite.

A result of subtraction

B result of dilation

Once the segmentation of the microstructural elements of the white cast iron being analyzed has been accomplished, the system identifies and quantifies those elements using the artificial neuronal network.

In Figure 11, the pearlite (represented in green) and cementite (represented in yellow) elements quantified by the ANN are visible. The values obtained are 51.93% for pearlite and 48.07% for cementite. The quantification of ledeburite microstructure is obtained from Figure 12.

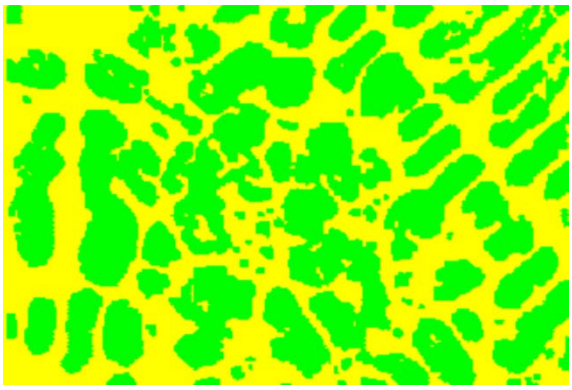

Fig. 11 Result of the identification and quantification of the pearlite and cementite elements from the proposed system.

It is important to mention that the cementite percentage obtained includes the constituent ledeburite, which it is not correct. To solve this, it is necessary to quantify the ledeburite, and then deduct it from the percentage of cementite previously obtained.

Figure 12 presents the image after the quantification of the constituent ledeburite by the artificial neural network. In the present case, the constituent ledeburite was 9.2%.

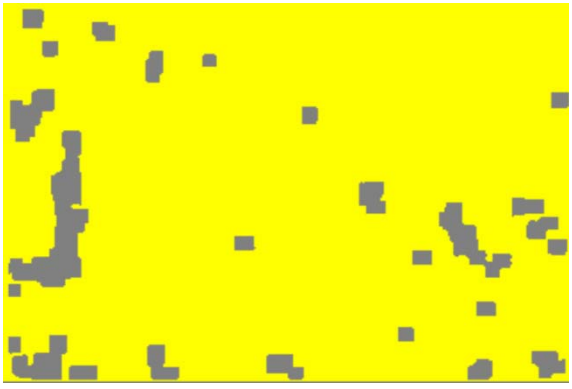

Fig. 12 Result of the identification and quantification of ledeburite using the proposed system.

Thus, for the sample considered in this section, the final estimates of the percentages of pearlite, cementite and ledeburite were equal to 51.93%, 38.87% and 9.2%, respectively.

The results for the other 29 samples were very similar to the ones described in this section. Furthermore, the segmentations were always very similar to the ones accomplished by an experienced operator through visual inspection and the quantification results were consistent for all samples.

6. Conclusions

This paper describes a new computational system developed for segmentation, identification and quantification of microstructural elements of metallic materials from images that uses mathematical morphology and an ANN.

An experimental analysis was carried out, using the proposed system for the segmentation and quantification of microstructural elements, on 30 samples of a white cast iron. The time needed to accurately perform the segmentation and quantification of one metallographic image using our system is around 3 minutes, including the image acquisition step, and around 2.5 to 3 hours by the usual manual analysis. It should be noted that the accurate quantification by visual inspection is impossible, since the microstructures of hypoeutectic white cast irons are morphologically very complex.

In the case of white cast iron, it is necessary to emphasize once more the importance of the application of an adequate threshold level in the binarization of the input image to be analyzed. In the computational system developed, this threshold value is automatically obtained through the determination of the lowest peak located in the valley that is characteristic of white cast irons.

Using the proposed computational system for several metallographic experiments, as well as with different metallic samples, we verified that it can be satisfactorily used to segment and quantify microstructural constituents from images. In relation to other software available, the main advantage is the considerable reduction in the time spent to quantify the constituents of

the material being analyzed, as well as the possibility of obtaining better-quality segmentations. Other advantages are the ease of use and the robustness of the ANN employed to the noise that input images may contain caused mainly by optical distortions or irregularities of the lighting conditions during the acquisition process.

From the analysis of the experimental results obtained, one may conclude that the proposed system is very efficient and more than adequate for the level usually required for Material Sciences domain. It can be used by researchers, engineers, specialists and others, as a valid tool to optimize the segmentation and quantification process of microstructural elements of metallic material from images.

Acknowledgments

The authors would like to express their deep gratitude to David Graham Straker for his valuable help in reviewing the English version of this paper.

The authors would like to thank also to the Brazilian research agency CNPq - The National Council for Scientific and Technological Development for the financial support.

7. References

Abdelhay, A. (2005) 'Application of artificial neural networks to predict the carbon content and the grain size for carbon steels', Egyptian Journal of Solids, Vol. 25, pp. 229-243.

Albuquerque, V.H.C. de, Alexandria, A.R. de, Cortez, P.C., Tavares, J.M.R.S. (2009) 'Evaluation of multilayer perceptron and self-organizing map neural network topologies applied on microstructure segmentation from metallographic images'. NDT & E International. Vol 42, 644-651.

Albuquerque, V.H.C., Cortez, P.C., Alexandria, A.R. and Tavares, J.M.R.S. (2008) ‘A new solution for automatic microstructures analysis from images based on a backpropagation artificial neural network’, Nondestructive Testing and Evaluation, Vol. 23, pp. 273-283.

Bhadeshia, H.K.D.H. (1994) ‘Neural networks and genetic algorithms in materials science and engineering’, India: Tata McGraw-Hill Publishing Company Ltd..

Bhadeshia, H.K.D.H. (1999) ‘Neural networks in materials science’, ISIJ International, Vol. 39, pp. 966-979.

Biernacki, R., Kozłowski, J., Myszka, D. and Perzyk, M. (2006) ‘Prediction of properties of austempered ductile iron assisted by artificial neural network’, Materials Science (Medžiagotyra), Vol. 12, pp. 11-15.

Callister, W. (2006) ‘Materials science and engineering: an introduction’, New York: John Wiley & Sons Inc.

Gonzalez, R.C. and Woods, R.E. (2008) ‘Digital Image Processing’ New York: Addison-Wesley Publishing Company.

Haykin, S. (1994) ‘Neural networks: a comprehensive foundation’, New York: Macmillan College Publishing Company Inc.

Kim, I., Jeong, Y., Lee, C. and Yarlagadda, P. (2003) ‘Prediction of welding parameters for pipeline welding using an intelligent system’, The International Journal of Advanced Manufacturing Technology, Vol. 22, pp. 713-719.

Kusiak, J. and Kuziak, R. (2002) ‘Modelling of microstructure and mechanical properties of steel using the artificial neural network’, Journal of Materials Processing Technology, Vol. 127, pp. 115-121.

Li, X. and Miaoquan, L. (2005) ‘Microstructure evolution model based on deformation mechanism of titanium alloy in hot forming’, Transactions of non ferrous metals society of China, Vol. 15, pp. 749-753.

Miaoquan, L., Liu, X., Xiong, A. and Li, X. (2002) ‘An adaptive prediction model of grain size for the forging of Ti-6Al-4V alloy based on the fuzzy neural networks’, Journal of Materials Processing Technology, Vol. 123, pp. 377-381.

Miaoquan, L., Liu, X., Xiong, A. and Li, X. (2003) ‘Microstructural evolution and modelling of the hot compression of a TC6 titanium alloy’, Materials Characterization, Vol. 49, pp. 203-209.

Samarasinghe, S. (2006) ‘Neural networks for applied sciences and engineering: from fundamentals to complex pattern recognition’, London: Auerbach Publications.

Wang, O., Lai, J. and Sun, D. (2007) ‘Artificial neural network models for predicting flow stress and microstructure evolution of a hydrogenized titanium alloy’, Key Engineering Materials, Vol. 358, pp. 541-544.